# In Silico and In Vivo Approach to Elucidate the Inflammatory Complexity of CD14-deficient Mice

Jose M Prince,[1] Ryan M Levy,[1] John Bartels,[2] Arie Baratt,[2] John M Kane, III,[1] Claudio Lagoa,[1] Jonathan Rubin,[3,5] Judy Day,[3] Joyce Wei,[2] Mitchell P Fink,[1,4,5] Sanna M Goyert,[6] Gilles Clermont,[4,5] Timothy R Billiar,[1,5] and Yoram Vodovotz[1,5,7]

[1]Department of Surgery, University of Pittsburgh, Pittsburgh, PA, USA; [2]Immunetrics, Inc., Pittsburgh, PA, USA; [3]Department of Mathematics, University of Pittsburgh, Pittsburgh, PA, USA; [4]Department of Critical Care Medicine, University of Pittsburgh, Pittsburgh, PA, USA; [5]McGowan Institute for Regenerative Medicine, Center for Inflammation and Regenerative Modeling, University of Pittsburgh, Pittsburgh, PA, USA; [6]North Shore-Long Island Jewish Research Institute/New York University School of Medicine, Manhasset, NY, USA; [7]Department of Immunology, University of Pittsburgh, Pittsburgh, PA, USA

The inflammatory phenotype of genetically modified mice is complex, and the role of Gram-negative lipopolysaccharide (LPS) in acute inflammation induced by surgical cannulation trauma, alone or in combination with hemorrhage and resuscitation ("hemorrhagic shock"), is both complex and controversial. We sought to determine if a mathematical model of acute inflammation could elucidate both the phenotype of CD14-deficient ($CD14^{-/-}$) mice—following LPS, cannulation, or hemorrhagic shock—and the role of LPS in trauma/hemorrhage-induced inflammation. A mathematical model of inflammation initially calibrated in wild-type (C57Bl/6) mice subjected to LPS, cannulation, and hemorrhagic shock was recalibrated in $CD14^{-/-}$ mice subjected to the same insults, yielding an ensemble of models that suggested specific differences at the cellular and molecular levels (for example, 43-fold lower activation of leukocytes by LPS). The $CD14^{-/-}$-specific model ensemble could account for complex changes in inflammatory analytes in these mice following LPS treatment. Model prediction of similar organ damage in $CD14^{-/-}$ and wild-type mice subjected to cannulation alone or with hemorrhagic shock was verified in vivo (similar ALT levels). These studies suggest that LPS-CD14 responses do not cause inflammation in surgical trauma/hemorrhagic shock and demonstrate a novel use of combined in silico and in vivo methods to elucidate the complex inflammatory phenotype of genetically modified animals.

## INTRODUCTION

Trauma and its sequelae remain the leading cause of death in the United States for individuals younger than 54 y (1). Approximately 50% of patients die early due to multiple organ failure (MOF) and other consequences of head injury or hemorrhagic shock (HS) (1). MOF is thought to be caused, at least partially, by excessive or maladaptive activation of inflammatory pathways, leading to generalized dysregulation of homeostatic mechanisms initiated by tissue trauma and HS (1). Though many organs are affected by the systemic mediators released during HS, the liver and gut are primary sites of response following hemorrhagic shock (1).

The events that initiate the inflammatory response in HS are complex, interrelated, and highly redundant. This complexity is, in part, the reason for the paucity of therapeutic options in sepsis and trauma (2-6). We have developed a series of mathematical models of increasing complexity in their mechanistic description of the dynamics of cellular and molecular effectors of inflammation, in an attempt to address the complexity of acute inflammation (7-9). The most complete model predicts the time course of key mediators of innate immunity in C57Bl/6 mice subjected to intraperitoneal injection of bacterial lipopolysaccharide (LPS), surgical trauma consisting of the insertion of cannulae without further intervention (cannulation), and cannulation followed by hemorrhagic shock and resuscitation (hemorrhagic shock) (9). Despite having been calibrated on nonlethal doses of LPS, this mathematical model could predict doses of LPS at which mice are known to die. Although the model has been constructed substantially using measured plasma levels of circulating mediators, it expresses the physiological derangement experienced by individual organs in terms of a global "tissue dysfunction" equation (7-9). Damage/dysfunction serves as an indicator of the host's health as well as being an inducer of inflammation (analogous to endogenous "danger signals") (10).

Two issues that affect the field of mathematical modeling of complex biological systems are 1) the ability of the models to settle biological controversies (11) and 2) the imprecise mechanisms by

Address correspondence and reprint requests to Yoram Vodovotz, University of Pittsburgh, Department of Surgery, W944 Biomedical Science Tower, 200 Lothrop St, Pittsburgh, PA 15213. Phone: (412) 647-5609; fax: (412) 383-5946; e-mail: vodovotzy@upmc.edu.

which modelers settle on a single model that describes a biological process (6,12). We sought to address the first point by using our model to elucidate controversial issues in acute inflammation. One such issue is the role of LPS translocation in cannulation- or hemorrhagic shock–induced inflammation. The intestine is highly sensitive to ischemia-reperfusion injury and experiences a marked reduction in blood flow during circulatory shock, due to a disproportionate constriction of the splanchnic circulation. Several studies have proposed that many of the inflammatory changes characteristic of cannulation or hemorrhagic shock are secondary to the release and recognition of gut-derived immunostimulants such as LPS, or following bacterial translocation due to increased intestinal permeability (13-23). Nonetheless, both animal (24) and clinical (25-27) studies have failed to implicate LPS or bacterial translocation in this process.

We sought to address the second modeling issue by following a practice developed in the field of weather forecasting, known as "ensemble modeling." In ensemble modeling, 5 to 100 different models of the same process are, in aggregate, capable of more accurate forecasts than any one given model (28). We chose to carry out this process in mice deficient in CD14. The initial recognition of LPS occurs primarily through binding to LPS binding protein (LBP) in plasma, which presents LPS to cells that recognize the complex through the CD14-TLR4 receptor complex (29-32). Although CD14 has been used for monitoring the status of trauma patients (33,34), the role of this molecule is unclear (35). We created an ensemble of possible models fit to data in mice deficient in CD14 and analyzed the predictions of the model compared with actual data obtained in CD14-deficient ($CD14^{-/-}$) mice.

The studies described herein suggest that LPS does not mediate cannulation or hemorrhagic shock–induced inflammation via the classic CD14-TLR4 pathway. Furthermore, we demonstrate for the first time that a mathematical model of the acute inflammatory process (9)—

combined with methodology previously used only in numerical weather forecasting [ensemble modeling (28)], automated fitting algorithms, and easily measurable circulating inflammatory analytes—can be used to yield mechanistic information about mice deficient in key inflammation-associated molecules. In a larger context, we are describing a novel approach that may also be used to rapidly generate a series of plausible variants of a "baseline" mathematical model, a process that may be applied to gain novel insight into the biological mechanisms of perturbations such as drug treatment.

## MATERIALS AND METHODS

### Mathematical Model of Acute Inflammation

The equations and specifications (Table S1, supplementary materials) of the mathematical model of inflammation have been described elsewhere (9). $CD14^{-/-}$-specific changes are depicted in Table S2 (supplementary materials). Briefly, we constructed a mathematical model of acute inflammation that incorporates key cellular and molecular components of the acute inflammatory response. The mathematical model consists of a system of 17 nonlinear ordinary differential equations that describe the time course of these components. Included in the model equations are 2 systemic variables that represent mean arterial blood pressure and global tissue dysfunction and damage. "Global tissue damage/dysfunction" describes the overall health of the organism, because the hallmark of all physiological derangements accompanying sepsis and hemorrhagic shock is the eventual, sequential failure of multiple organs. Given the complexity of simulating individual organs, we approximated this process by treating it as a gradual, ongoing process occurring in the whole body and driven by inflammation. Thus, elevated and unrecoverable tissue damage/dysfunction served as a surrogate for death, whereas damage/dysfunction that tended to return to baseline over time was a proxy for sur-

vival. In the model, LPS, cannulation, and hemorrhagic shock are all initiators of inflammation. We note that hemorrhagic shock is caused after cannulation injury that disrupts the integrity of blood vessels, and thus the 2 processes must be accounted for in an accurate simulation.

Each equation was constructed from known interactions among model components as documented in the existing scientific literature. The model and parameters were specified in 3 stages. In the preliminary stage, the model was constructed so that it could reproduce qualitatively several different scenarios reported in the literature. In this stage, experimentally determined values of parameters such as cytokine half-lives were used when available. In the second stage, the model was matched to our experimental data by adjusting some of the parameters using our qualitative understanding of the biological mechanisms together with the dynamics of the model, to attain desired time course shapes. In the third stage, the parameters were optimized by fitting the model to the experimental data and using a stochastic gradient descent algorithm that was implemented in Immunetrics, Inc. software (Pittsburgh, PA). We also used these algorithms to modify the mathematical model to account for inflammation in $CD14^{-/-}$ mice, as follows. We sought to find a minimal number of parameter changes that would allow our original model to accurately reproduce empirically observed time courses in $CD14^{-/-}$ mice. To prevent the optimizing algorithm from exploiting the indirect action of unmeasured analytes, we attempted to confine our search to those parameters that appear directly in the equations of our measured analytes (TNF, IL-6, IL-10, $NO_2^-/NO_3^-$). Our procedure was to impose a limit of $n$ changes, run an optimizer bounded by this change limit, and evaluate the fit. We evaluated these fits with respect to quantitative error totals as well as general qualitative behavior. After evaluation, we increased the number of parameters to be optimized and repeated the process iteratively until

sufficient fit quality was achieved. Each optimization pass was allowed to randomly choose which $n$ of the candidate parameters to change. We performed numerous fits for each $n$ to account for the stochastic nature of our gradient descent search. To obtain good fits with fewer than 10 changes, we found it necessary to add the parameters of the (unmeasured) MA, NA, and iNOS equations to our initial set of parameters to be fitted (see supplementary materials) (9). When these parameters were included in the search, we found that excellent fits could be obtained with 8 parameter changes. We also observed that eliminating any 1 of these changes seems to result in a worse fit by both quantitative and qualitative measures. This procedure yielded 5 parameter sets with good fits to the data in CD14⁻/⁻ mice, with essentially equal measures of error with respect to experimental data (data not shown). The models exhibited similar behavior with regard to model output (Figures 1-3) and predictions (Figure 4) presented herein, with various tradeoffs relative to a hypothetical perfect fit. Each parameter set was based on similar, but not identical, changes to various constants (Table S2). We show these models and indicate the one judged as the best overall fit to the data by investigator consensus (necessary given the overall similarity of the quantitative measures used to possibly distinguish among the models). Nonetheless, the model output and predictions of all models are shown.

### Reagents

All reagents were from Sigma Chemical Co. (St. Louis, MO, USA) unless otherwise indicated.

### Animals

Mice used in the experimental protocols were housed in accordance with NIH animal care guidelines after approval of the University of Pittsburgh Institutional Animal Care and Use Committee. All animals were maintained in specific pathogen–free conditions with 12-h light/dark facilities and received

food and water ad libitum. Male C57Bl/6 mice (8 to 12 weeks old, weighing 20 to 30 g) (Charles River, Wilmington, MA, USA) were used for the initial calibration of the mathematical model as described elsewhere (9). In addition, male CD14⁻/⁻ mice (36,37) (obtained both from S.M.G. and Dr. Mason Freeman, Massachusetts General Hospital, Boston, MA, USA) and corresponding CD14 wild-type mice were subjected to LPS, cannulation, or hemorrhagic shock. All animals were acclimated for 7 days before being used in experimental protocols.

### LPS Protocol

As described elsewhere (9), C57Bl/6 mice received 3, 6, or 12 mg/kg LPS from *E. coli* O111:B4 or saline control intraperitoneally. CD14⁻/⁻ mice received 3 mg/kg LPS intraperitoneally. At various time points after the injection, the mice (4 to 8 separate mice per time point) were killed and their serum obtained for measurement of various analytes (see below). All the mice survived the LPS dose until the final time point (24 h after injection).

### Cannulation and Hemorrhagic Shock Protocol

Animals were anesthetized with intraperitoneal sodium pentobarbital (50 mg/kg) supplemented with inhaled isoflurane (Abbott Labs, Chicago, IL, USA) when necessary. Both femoral arteries were cannulated with tapered PE-10 tubing. The catheters were flushed with heparin sulfate (Pharmacia & Upjohn, Kalamazoo, MI, USA) for an estimated total dose of 2 units per animal. One catheter was used for hemorrhage/resuscitation and the other was connected to a blood pressure transducer (Micro-Med, Tustin, CA, USA) for continuous mean arterial pressure readings. The mice were allowed to recover from the inhalational anesthesia for 10 min before initiation of HS. The hemorrhagic shock animals were treated as follows. After baseline blood pressure readings, repeated 3 times, the mice were subjected to hemorrhagic shock by withdrawal of blood (2.25 mL/100 g body weight) over 10 min to achieve a mean

arterial pressure (MAP) of 25 mmHg. MAP was maintained at 25 mmHg for 2.5 h with continuous monitoring of blood pressure and withdrawal and return of blood as needed. After 2.5 h, the mice were resuscitated over 20 min with their remaining shed blood plus 2 times the maximal shed blood volume of lactate Ringer's solution. The cannulae were then removed, and the bilateral groin incisions were closed. Animals were allowed to recover from anesthesia and were then returned to their cages with free access to water. Cannulation-only animals underwent anesthesia and femoral cannulation only. Animals were killed under excess inhalational anesthesia 4 h after the initiation of resuscitation (6.5 h from start of experiment). Plasma from post-mortem blood samples was obtained for cytokine and blood chemistry analysis as described below.

### Analysis of Cytokines, NO₂⁻/NO₃⁻, and Alanine Aminotransferase

TNF, IL-10, and IL-6 were measured using commercially available ELISA kits (R&D Systems, Minneapolis, MN, USA). Nitric oxide was measured as $NO_2^-$/$NO_3^-$ by the nitrate reductase method (38) using a commercially available kit (Cayman Chemical, Ann Arbor, MI, USA). Alanine aminotransferase (ALT) was measured using a commercially available kit (Vitros Chemistry; Ortho-Clinical Diagnostics, Raritan, NJ, USA) according to manufacturer's instructions.

### RESULTS

### Mathematical Modeling Acute Inflammation in C57Bl/6 and CD14⁻/⁻ Mice

We constructed a mathematical model that incorporates known physiological interactions between the various elements of the immune system (9) (see also supplementary materials). The model was calibrated to experimental data sets obtained in male wild-type (C57Bl/6) mice in 5 scenarios of inflammation: LPS intraperitoneal injection (3 mg/kg, 6 mg/kg, and 12 mg/kg); cannulation; and hemor-
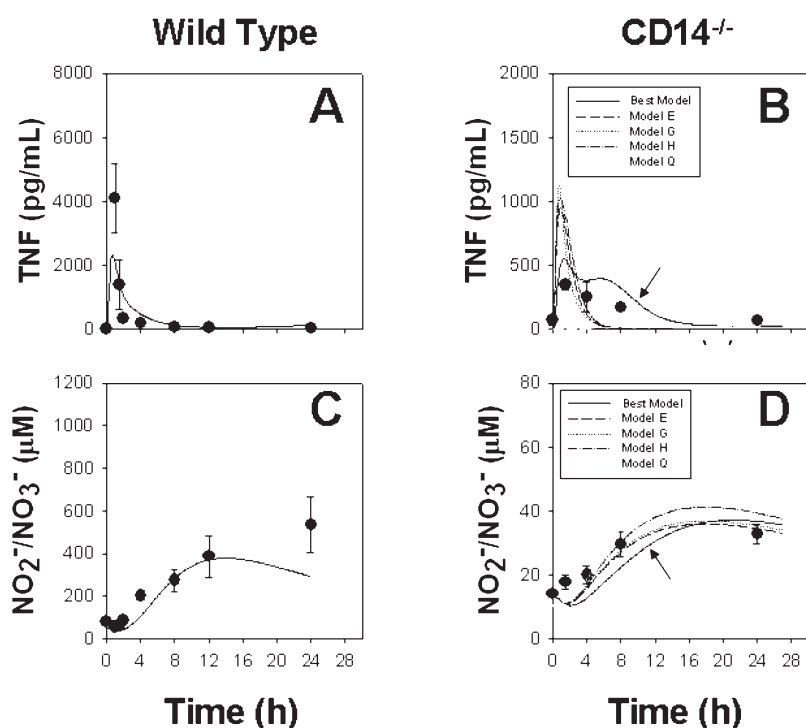
**Figure 1.** Data and model output for plasma TNF and $NO_2^-/NO_3^-$ in wild-type and $CD14^{-/-}$ mice subjected to LPS. Wild-type (C57Bl/6; 3-8 per time point) and $CD14^{-/-}$ (4 per time point) mice were injected with 3 m/kg of *E. coli* LPS. TNF and $NO_2^-/NO_3^-$ (symbols, showing mean ± SEM) were measured as described in "Materials and Methods." For wild-type mice (A and C), the line indicates the output of the baseline (wild-type) model of acute inflammation (9). For $CD14^{-/-}$ mice (B and D), model recalibration was carried out as described in "Materials and Methods," yielding an ensemble of 5 models (lines). "Best Model" indicates the model giving the best overall qualitative fit to the data as judged by investigator consensus.

rhagic shock. Four analytes—TNF, IL-10, IL-6, and stable reaction products of NO ($NO_2^-/NO_3^-$)—were measured in all scenarios. These analytes were chosen because they represent a diverse selection of the main responders of the early inflammatory response and are produced on a rapid (TNF, IL-10), intermediate (IL-6), and slow ($NO_2^-/NO_3^-$) time scale. Thus, the mathematical model was partially calibrated with regard to inflammation induced both by LPS and by trauma/hemorrhage (9). Importantly, the damage/dysfunction variable in our model was not calibrated with respect to death/survival outcome, because in all the calibration scenarios the inflammation induced was nonlethal. Previously, predictions of damage/dysfunction were used as a test of the model, in that the damage/

dysfunction variable was used to predict a threshold dose of LPS above which mortality would occur (9). In the present study (see below), the damage/dysfunction variable was compared with circulating ALT as a global, circulating marker of organ damage.

In the cannulation and hemorrhagic shock scenarios, the model was able to match the data without the need to invoke an additional driver of inflammation in the form of LPS (9). This model structure was tantamount to a hypothesis for which there is both assenting and dissenting evidence (13-27). One goal of systems biology is to use mathematical modeling to address such controversies (11). Accordingly, we employed a novel modeling approach to test this hypothesis further. We modified, using automated algorithms, our

wild-type (C57Bl/6) mouse–specific mathematical model of inflammation to account for the levels of circulating inflammatory analytes in $CD14^{-/-}$ mice. This recalibration was followed by predictions and in vivo validation of damage/dysfunction in $CD14^{-/-}$ mice subjected to cannulation or hemorrhagic shock.

Although various naturally LPS-hyporesponsive mouse strains exist (for example, the TLR4-mutant C3H/HeJ strain), we chose to use $CD14^{-/-}$ mice. We have recently shown that C3H/HeJ mice also mount a smaller inflammatory response in response to ischemia/reperfusion injury, owing to injury-mediated release of HMGB1 whose effects are mediated via TLR4 (39). Male $CD14^{-/-}$ mice were subjected to LPS at 3 mg/kg. Plasma TNF, IL-6, IL-10, and $NO_2^-/NO_3^-$ were assessed at various time points. As seen in Figure 1, TNF (compare A and B) and $NO_2^-/NO_3^-$ (compare C and D) were produced at nearly 10-fold lower levels in $CD14^{-/-}$ mice compared with C57Bl/6 mice. The time course of IL-6 production was subtly different in the 2 strains. $CD14^{-/-}$ mice exhibited a more rapid decay of IL-6 levels compared with C57Bl/6 mice (Figure 2, compare A and B). Surprisingly, we found that the dynamics of IL-10 were essentially identical in $CD14^{-/-}$ and C57Bl/6 mice (Figure 2, compare C and D).

We next subjected C57Bl6/ and $CD14^{-/-}$ mice to cannulation alone or hemorrhagic shock, and examined IL-6 (Figure 3A) and IL-10 (Figure 3B) levels. Due to sample size limitations, TNF and $NO_2^-/NO_3^-$ could not be measured. The data from $CD14^{-/-}$ mice were used recalibrate the mathematical as described in "Materials and Methods." We created an ensemble of 5 models, each model the product of an independent recalibration of our baseline (C57Bl/6-specific) mathematical model to the data in $CD14^{-/-}$ described above (Table S2 in supplementary materials). This approach, previously used in weather forecasting (28), to our knowledge has not previously been used in modeling biological systems. The $CD14^{-/-}$-specific models had some parameter changes in common, while hav-
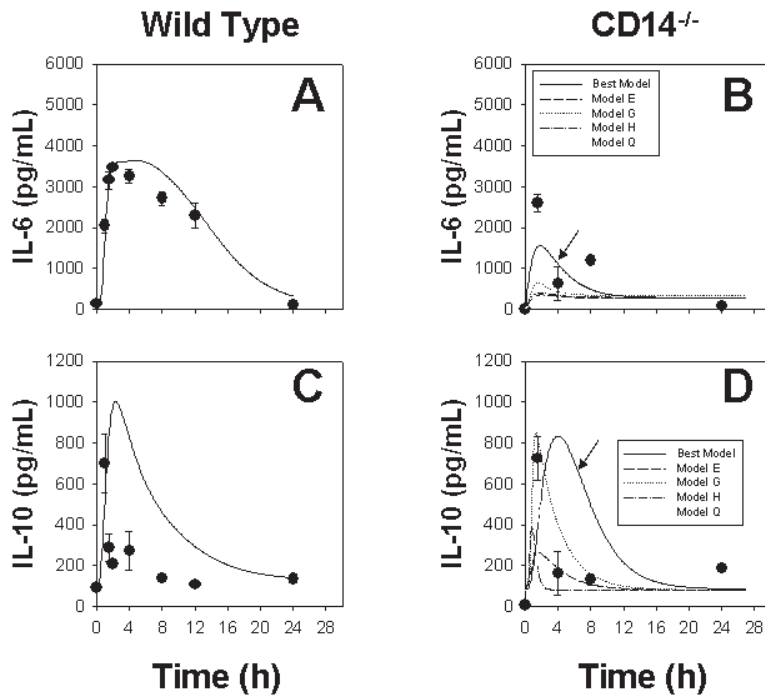
**Figure 2.** Data and model output for plasma IL-6 and IL-10 in wild-type and CD14$^{-/-}$ mice subjected to LPS. Wild-type (C57Bl/6; 3-8 per time point) and CD14$^{-/-}$ (4 per time point) mice were injected with 3 m/kg of *E. coli* LPS. IL-6 and IL-10 (symbols, showing mean ± SEM) were measured as described in "Materials and Methods." For wild-type mice (A and C), the line indicates the output of the baseline (wild-type) model of acute inflammation (9). For CD14$^{-/-}$ mice (B and D), model recalibration was carried out as described in "Materials and Methods," yielding an ensemble of 5 models (lines). "Best Model" indicates the model giving the best overall qualitative fit to the data as judged by investigator consensus.

ing very different parameter changes in some cases (Table S2 in supplementary materials). The output of our previously published, wild-type (C57Bl/6) mouse–specific model (9) is depicted as the lines in Figures 1A/C and 2A/C, and as the black bars in Figure 3A/B. The output of the CD14$^{-/-}$-specific ensemble is depicted as the lines in Figures 1B/D and 2B/D and as the white bars in Figure 3A/B. In the case of the CD14$^{-/-}$-specific model, we refer to the predictions of the ensemble as a whole, though we also designated 1 model as the "best" model based on overall visual fit to the data. We did this because in most studies involving modeling of biological systems, a single "best" model is generated following some combination of quantitative and qualitative procedures. In Figures 1 and 2, we show the dynamics of the 5 models

that fit our criteria; the "best" is indicated in the solid line (arrows). In Figure 3, the variability in output of these models is shown as the standard error for each predicted analyte. Importantly, this recalibration was based on a small set of changes to the baseline model (see "Materials and Methods" and Table S2 of supplementary materials).

The changes (relative to the C57Bl/6-specific model) in the CD14$^{-/-}$-specific model ensemble included both ones that would have been chosen intuitively (for example, decreased responsiveness of leukocytes to LPS) and others that were not intuitively obvious (for example, altered IL-6, IL-10, and NO production; see Table S2). Moreover, we note that the CD14$^{-/-}$-specific model, like the C57Bl/6 base model, did not invoke LPS release in cannulation- or hemorrhagic shock–

induced inflammation. Importantly, we compared wild-type littermates of CD14$^{-/-}$ mice to C57Bl/6 mice with regard to their systemic levels of IL-6 and IL-10 in response to cannulation or hemorrhagic shock. These levels did not differ in a statistically significant fashion (data not shown).

## Mathematical Prediction of Organ Damage and In Vivo Validation

Organ damage data were not used for the calibration of the CD14$^{-/-}$-specific model. Instead, we used organ damage data to validate the C57Bl/6- and CD14$^{-/-}$-specific mathematical models. As a marker of organ damage, we used circulating ALT, an accepted marker of liver damage in surgical trauma without and with hemorrhagic shock (40). Both the wild-type– and CD14$^{-/-}$-specific models predicted elevations of damage/dysfunction in response to hemorrhagic shock compared with cannulation. Additionally, the levels of damage/dysfunction were predicted to be similar between wild-type and CD14$^{-/-}$ mice for the same insult (Figure 4A; standard error indicates variability of the 5 models). Indeed, ALT levels were elevated in hemorrhagic shock compared with cannulation only in both C57Bl/6 and CD14$^{-/-}$ mice to a similar extent (Figure 4B). Further supporting the models' prediction were data demonstrating 1) no difference in baseline MAP between the experimental groups; 2) a similar hemodynamic response to the hemorrhage procedure in wild-type and CD14$^{-/-}$ mice subjected to surgical trauma without and with hemorrhagic shock, with no significant differences in the total volume of blood removed or time required to attain the target MAP of 25 mmHg; 3) a stable MAP throughout the experimental period in both wild-type and CD14$^{-/-}$ animals subjected to cannulation only; and 4) zero mortality for all experimental groups.

*Please note that supplementary information is available on the Molecular Medicine website (www.molmed.org).*
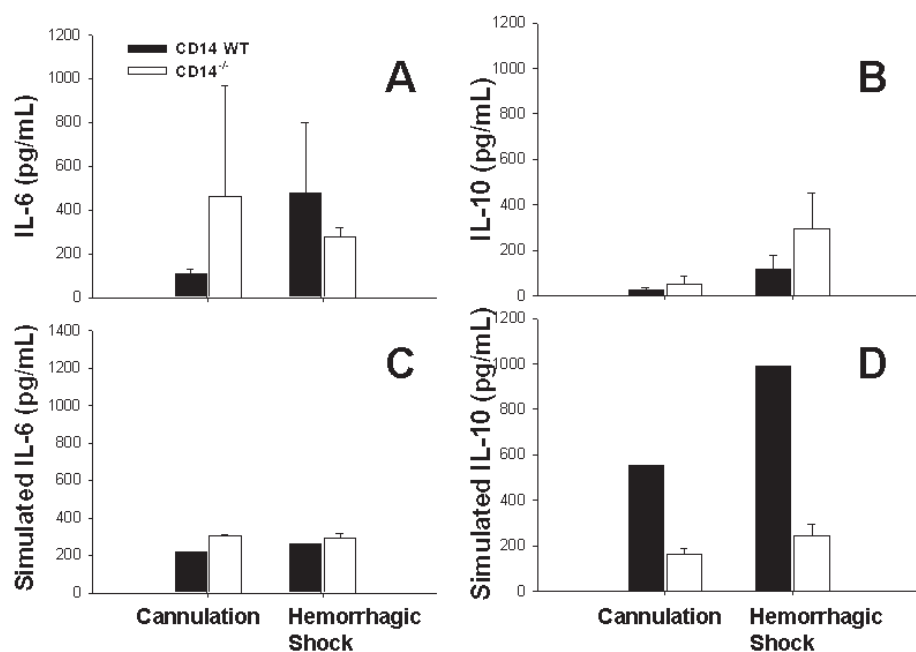
**Figure 3.** Data and model output for plasma IL-6 and IL-10 in wild-type and CD14$^{-/-}$ mice subjected to cannulation or hemorrhagic shock. Wild-type (C57Bl/6; 7 per time point) and CD14$^{-/-}$ (5 per time point) mice were subjected to cannulation or hemorrhagic shock as described in "Materials and Methods." IL-6 (A) and IL-10 (B) were measured as described in "Materials and Methods" and are shown as mean ± SEM. Black bars: wild-type mice; open bars: CD14$^{-/-}$ mice. C and D indicate the output of the ensemble of mathematical models, showing simulated levels of IL-6 and IL-10, respectively. Black bars: output of baseline (wild-type) model of inflammation (9); open bars, output of the ensemble of 5 CD14$^{-/-}$-specific models of inflammation (shown as mean ± SEM).

## DISCUSSION

Mathematical modeling is emerging as a novel approach by which to address the complexity inherent in inflammation and associated processes (2,4,6). One key use of mathematical modeling is to address biological controversies (11). We carried out a combined program of systematic data collection and model recalibration in mice deficient in their response to LPS via the classic CD14-dependent pathway, to test the hypothesis that LPS release was not necessary to account for cannulation- or hemorrhagic shock–induced inflammation. Our results suggest that a response to LPS is not necessary to account for inflammation induced by trauma/hemorrhage.

We also addressed in the present study a little-discussed issue in the field of biological modeling that concerns the ability to fully specify a single model that accurately describes the biology in question (6,12). Without very much data, it is essentially impossible to fully specify the parameters of a mathematical model such as ours. We suggest that there are always multiple models that can produce comparable predictions while invoking markedly different mechanisms or balances in tuning. To address this problem, and also to improve the predictive ability of the model, we have turned to ensemble modeling (28). The principal value of the ensemble is to highlight the spectrum of possible explanations for a set of biological observations (for example, the differences in the levels of inflammatory mediators in wild-type vs. CD14$^{-/-}$ mice). Concordance between the ensemble members with regard to changes from the baseline (wild type) model strongly suggests that the model leaves only one way to achieve a given set of results.

Different explanations among ensemble members for a divergence from the wild type would lead to 1 of 2 possible conclusions. The first possibility is that the ensemble explanations diverge from known biological observations, in which case specific mechanisms in the model might require revision. Alternatively, there may really be multiple possible ways to realize the target data. Our automated recalibration procedure (detailed in "Materials and Methods") yielded an ensemble of 5 models with relatively similar fit to circulating TNF, IL-6, IL-10, and $NO_2^-$/$NO_3^-$ levels in CD14$^{-/-}$ mice (Figures 1-3; Table S2). These CD14$^{-/-}$-specific models shared some features and differed in others (Table S2). However, all of the models predicted damage/dysfunction in response to cannulation alone or with hemorrhagic shock that was similar not only among CD14$^{-/-}$-specific models but also to the damage dysfunction predicted and observed in wild-type mice (Figure 4). Because we did not include LPS release post-trauma/hemorrhage in any of these CD14$^{-/-}$-specific models, none of the models could invoke a response to endogenous LPS to account for the dynamics of inflammatory mediators and organ damage/dysfunction. This finding strengthens our conclusion regarding the lack of a role for the classic LPS-CD14 pathway in inflammation and organ damage after cannulation or hemorrhagic shock.

We stress that the conclusions we make were derived from the ensemble of models, rather from any single model. The models that make up the CD14$^{-/-}$ ensemble share certain features and differ in others (Table S2) and were essentially indistinguishable based on quantitative features. In most studies employing the creation of mathematical models of complex biological systems, only a single model is reported and that typically some sort of qualitative, visual fit to the data is employed along with quantitative measures. The "best model" that was selected following the CD14$^{-/-}$-specific recalibration procedure (judged qualitatively by visual fit to the calibration data)
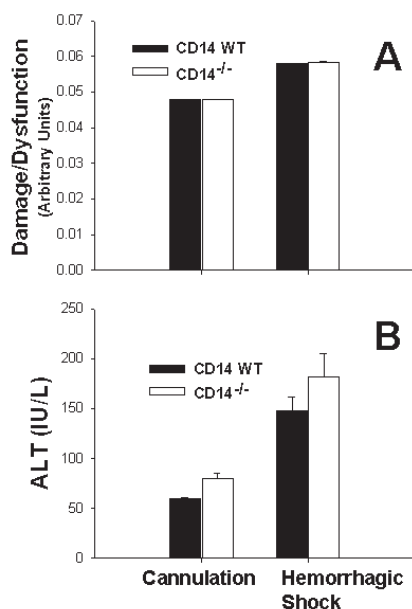
**Figure 4.** Data and model prediction for organ damage in wild-type and CD14$^{-/-}$ mice subjected to cannulation or hemorrhagic shock. Wild type (C57Bl/6; 7 per time point) and CD14$^{-/-}$ (5 per time point) mice were subjected to cannulation or hemorrhagic shock as described in "Materials and Methods." Predicted organ damage/dysfunction (A) is shown for the baseline model inflammation (9) (black bars) and the CD14$^{-/-}$-specific ensemble of 5 models (open bars; output of 5 models shown as mean ± SEM). Plasma ALT levels (B) were measured as described in "Materials and Methods" and are shown as mean ± SEM.

remarkably suggested several known changes in the inflammatory response of CD14$^{-/-}$ mice. These changes included reduced LPS responsiveness of leukocytes, as expected (36,37), as well as changes in IL-6, IL-10, and NO physiology (Table S2).

The controversy in the literature regarding the role of LPS in trauma/hemorrhage-induced inflammation may stem from the recently recognized ability of TLR4 to respond to ligands other than LPS (41-46). For example, DeMaria et al. (47) studied surgical trauma without and with hemorrhagic shock in C3H/HeJ (TLR4-mutant) and C3H/HeN (wild-type) mice and found reduced inflamma-

tory responses in the LPS-tolerant C3H/HeJ strain. Although these results appear puzzling at first in light of the responses shown here for CD14$^{-/-}$, we have recently shown that TLR4-mutant mice mount a smaller inflammatory response in response to ischemia/reperfusion injury owing to injury-mediated release of HMGB1 and subsequent signaling via TLR4 (39); we have observed similar responses of TLR4-mutant mice in the settings of hemorrhagic shock (48) and bilateral femur fracture (49). Indeed, a unifying theme in our mathematical models of acute inflammation is the feed-forward effect of tissue damage on inflammation and the reciprocal effect of inflammation on damage (7-9). The present study supports the notion that CD14 does not act to induce or augment cannulation- or hemorrhagic shock–induced inflammation via the classic, CD14-dependent LPS recognition pathway. Despite this evidence, it is still possible that LPS could mediate trauma/hemorrhage-induced inflammation via other cell surface receptors, including CD11/CD18 (50), the acetylated-LDL receptors (51), or scavenger receptors (52). Further work would be necessary to examine the role of these possible pathways.

We note that although in general our baseline model of acute inflammation in C57Bl/6 mice matches the dynamics of various circulating analytes (9), there are cases in which specific analytes do not match well at a given time point (for example, Figure 3D); this is a limitation inherent to the use of a mathematical model that represents a simplification of the known mechanisms of acute inflammation (6,12). Our recalibration approach also suffers from several limitations. Several of the models, but not the best one, achieved good fits to the data (and ultimately predicted no change in organ damage induced by hemorrhagic shock) despite changes in parameters that stand in contrast to published studies. For example, some of the models (but not the best) invoked an increase in the death rate of neutrophils and macrophages (Table S2). This result stands in contrast

to studies demonstrating reduced inflammatory stimulus–induced apoptosis in CD14$^{-/-}$ macrophages (53), as well as the known role for CD14 in clearance of apoptotic cells (54). However, to the best of our knowledge there are no studies that describe the in vivo rates of leukocyte apoptosis in CD14$^{-/-}$ mice compared with wild-type counterparts. Thus, we suggest that investigator intervention is necessary to judge the quality of any model generated by these automated approaches.

We have sought to use our mathematical models of inflammation to address both fundamental and applied topics in the setting of sepsis and trauma (6,55). We have previously demonstrated that our model could account for the features of sepsis patients in a virtual clinical trial of anti-TNF antibodies in sepsis (8) and suggest inflammatory biomarkers for patients undergoing cardiopulmonary bypass (6). We have used the model to streamline animal use in experiments involving bone fracture along with hemorrhagic shock (56). The present study shows for the first time that we can use such a baseline mathematical model of inflammation calibrated with a robust dataset in mice, combined with a relatively limited amount of data in a genetically altered mouse, to yield an ensemble of models that yield essentially the same prediction regarding a given outcome (overall organ damage/dysfunction).

This striking observation of a high degree of concordance of outcome predictions from an ensemble of models raises the confidence level both in the predictions themselves and in possible practical uses of models such as ours. Our ultimate goal is to be able to use diverse preclinical data and baseline models in various species to model acute inflammation in humans, with the goal of improving drug design, clinical trials, and diagnostics. We suggest that this methodology could be used to describe and predict the actions of novel anti-inflammatory drugs in a given species and to use a model calibrated in one species to yield a model calibrated in another, closely related

species. We also suggest that the ensemble modeling method could be used in combination with mathematical models such as ours along with relevant biomarker data to create a diagnostic platform in the setting of sepsis and trauma.

## REFERENCES

1. Hierholzer C, Billiar TR. (2001) Molecular mechanisms in the early phase of hemorrhagic shock. *Langenbecks Arch. Surg.* 386:302-8.
2. Buchman TG, Cobb JP, Lapedes AS, Kepler TB. (2001) Complex systems analysis: a tool for shock research. *Shock* 16:248-51.
3. Neugebauer EA, Willy C, Sauerland S. (2001) Complexity and non-linearity in shock research: reductionism or synthesis? *Shock* 16:252-8.
4. Tjardes T, Neugebauer E. (2002) Sepsis research in the next millennium: concentrate on the software rather than the hardware. *Shock* 17:1-8.
5. Buchman TG. (2002) The community of the self. *Nature* 420:246-251.
6. Vodovotz Y, Clermont G, Chow C, An G. (2004) Mathematical models of the acute inflammatory response. *Curr. Opin. Crit. Care* 10:383-90.
7. Kumar R, Clermont G, Vodovotz Y, Chow CC. (2004) The dynamics of acute inflammation. *J. Theoretical Biol.* 230:145-55.
8. Clermont G, Bartels J, Kumar R, Constantine G, Vodovotz Y, Chow C. (2004) *In silico* design of clinical trials: a method coming of age. *Crit. Care Med.* 32:2061-70.
9. Chow CC et al. (2005) The acute inflammatory response in diverse shock states. *Shock* 24:74-84.
10. Gallucci S, Matzinger P. (2001) Danger signals: SOS to the immune system. *Curr. Opin. Immunol.* 13:114-9.
11. Kitano H. (2002) Systems biology: a brief overview. *Science* 295:1662-4.
12. An G. (2001) Agent-based computer simulation and SIRS: building a bridge between basic science and clinical trials. *Shock* 16:266-73.
13. Herman CM et al. (1972). Endogenous endotoxemia during hemorrhagic shock in the subhuman primate. *Surg. Forum* 23:14-5.
14. Woodruff PW, O'Carroll DI, Koizumi S, Fine J. (1973) Role of the intestinal flora in major trauma. *J. Infect. Dis.* 128, Suppl-4:
15. Herman CM et al. (1974) The relationship of circulating endogenous endotoxin to hemorrhagic shock in the baboon. *Ann. Surg.* 179:910-6.
16. Rhodes RS, DePalma RG, Robinson AV. (1975) Relationship of critical uptake volume to energy production and endotoxemia in late hemorrhagic shock. *Am. J. Surg.* 130:560-4.
17. Gaffin SL, Grinberg Z, Abraham C, Birkhan J, Shechter Y. (1981) Protection against hemorrhagic shock in the cat by human plasma containing endotoxin-specific antibodies. *J. Surg. Res.* 31:18-21.
18. Pohlson EC, Suehiro A, Ziegler EJ, Suehiro G, McNamara JJ. (1988) Antiserum to endotoxin in hemorrhagic shock. *J. Surg. Res.* 45:467-71.
19. Rush BF, Jr, Sori AJ, Murphy TF, Smith S, Flanagan JJ, Jr, Machiedo GW. (1988) Endotoxemia and bacteremia during hemorrhagic shock: the link between trauma and sepsis? *Ann. Surg.* 207:549-54.
20. Bahrami S, Schlag G, Yao YM, Redl H. (1995) Significance of translocation/endotoxin in the development of systemic sepsis following trauma and/or haemorrhage. *Prog. Clin. Biol. Res.* 392:197-208.
21. Guo W, Ding J, Huang Q, Jerrells T, Deitch EA. (1995) Alterations in intestinal bacterial flora modulate the systemic cytokine response to hemorrhagic shock. *Am. J. Physiol.* 269:G827-32
22. Jiang J, Bahrami S, Leichtfried G, Redl H, Ohlinger W, Schlag G. (1995) Kinetics of endotoxin and tumor necrosis factor appearance in portal and systemic circulation after hemorrhagic shock in rats. *Ann. Surg.* 221:100-6.
23. Shimizu T, Tani T, Hanasawa K, Endo Y, Kodama M. (2001) The role of bacterial translocation on neutrophil activation during hemorrhagic shock in rats. *Shock* 16:59-63.
24. Ayala A, Perrin MM, Meldrum DR, Ertel W, Chaudry IH. (1990) Hemorrhage induces an increase in serum TNF which is not associated with elevated levels of endotoxin. *Cytokine* 2:170-4.
25. Peitzman AB, Udekwu AO, Ochoa J, Smith S. (1991) Bacterial translocation in trauma patients. *J. Trauma* 31:1083-6.
26. Roumen RM, Hendriks T, Wevers RA, Goris JA. (1993) Intestinal permeability after severe trauma and hemorrhagic shock is increased without relation to septic complications. *Arch. Surg.* 128:453-7.
27. Endo S et al. (1994) Plasma endotoxin and cytokine concentrations in patients with hemorrhagic shock. *Crit. Care Med.* 22:949-55.
28. Gneiting T, Raftery AE. (2005) Atmospheric science: weather forecasting with ensemble methods. *Science* 310:248-9.
29. Beutler B, Hoebe K, Du X, Ulevitch RJ. (2003) How we detect microbes and respond to them: the Toll-like receptors and their transducers. *J. Leukoc. Biol.* 74:479-85.
30. Kitchens RL. (2000) Role of CD14 in cellular recognition of bacterial lipopolysaccharides. *Chem. Immunol.* 74:61-82.
31. Ingalls RR, Heine H, Lien E, Yoshimura A, Golenbock D. (1999) Lipopolysaccharide recognition, CD14, and lipopolysaccharide receptors. *Infect. Dis. Clin. North Am.* 13:341-53, vii.
32. Gangloff SC, Zahringer U, Blondin C, Guenounou M, Silver J, Goyert SM. (2005) Influence of CD14 on ligand interactions between lipopolysaccharide and its receptor complex. *J. Immunol.* 175:3940-5.
33. Grau GE, Mili N, Lou JN, Morel DR, Ricou B, Lucas R, Suter PM. (1996) Phenotypic and functional analysis of pulmonary microvascular endothelial cells from patients with acute respiratory distress syndrome. *Lab. Invest.* 74:761-70.
34. Heinzelmann M, Mercer-Jones M, Cheadle WG, Polk HC, Jr. (1996) CD14 expression in injured patients correlates with outcome. *Ann. Surg.* 224:91-6.
35. Omert L et al. (1998) A role of neutrophils in the down-regulation of IL-6 and CD14 following hemorrhagic shock. *Shock* 9:391-6.
36. Haziot A et al. (1996) Resistance to endotoxin shock and reduced dissemination of gram-negative bacteria in CD14-deficient mice. *Immunity.* 4:407-14.
37. Moore KJ et al. (2000) Divergent response to LPS and bacteria in CD14-deficient murine macrophages. *J. Immunol.* 165:4272-80.
38. Collins J, Vodovotz Y, Billiar TR. (2001) Biology of nitric oxide: measurement, modulation, and models. In *Surgical Research*. Souba W, WilmoreD, Eds. Academic Press, San Diego. p. 949-69.
39. Tsung A et al. (2005) The nuclear factor HMGB1 mediates hepatic injury after murine liver ischemia-reperfusion. *J. Exp. Med.* 201:1135-43.
40. Peitzman AB, Billiar TR, Harbrecht BG, Kelly E, Udekwu AO, Simmons RL. (1995) Hemorrhagic shock. *Curr. Probl. Surg.* 32:925-1002.
41. Vabulas RM, Ahmad-Nejad P, Ghose S, Kirschning CJ, Issels RD, Wagner H. (2002) HSP70 as endogenous stimulus of the Toll/interleukin-1 receptor signal pathway. *J. Biol. Chem.* 277:5107-12.
42. Smiley ST, King JA, Hancock WW. (2001) Fibrinogen stimulates macrophage chemokine secretion through toll-like receptor 4. *J. Immunol.* 167:2887-94.
43. Termeer C et al. (2002) Oligosaccharides of Hyaluronan activate dendritic cells via toll-like receptor 4. *J. Exp. Med.* 195:99-111.
44. Johnson GB, Brunn GJ, Kodaira Y, Platt JL. (2002) Receptor-mediated monitoring of tissue well-being via detection of soluble heparan sulfate by Toll-like receptor 4. *J. Immunol.* 168:5233-9.

45. Park JS, Svetkauskaite D, He Q, Kim JY, Strassheim D, Ishizaka A, Abraham E. (2004) Involvement of toll-like receptors 2 and 4 in cellular activation by high mobility group box 1 protein. *J. Biol. Chem.* 279:7370-7.

46. Tsung A et al. (2005) The nuclear factor HMGB1 mediates hepatic injury after murine liver ischemia-reperfusion. *J. Exp. Med.* 201:1135-43.

47. DeMaria EJ, Pellicane JV, Lee RB. (1993) Hemorrhagic shock in endotoxin-resistant mice: improved survival unrelated to deficient production of tumor necrosis factor. *J. Trauma.* 35:720-4.

48. Prince JM, Levy RM, Yang R, Mollen KP, Fink MP, Vodovotz Y, Billiar TR. (2006) Toll-like receptor-4 signaling mediates hepatic injury and systemic inflammation in hemorrhagic shock. *J. Am. Coll. Surg.* 202:407-17.

49. Levy RM et al. (2006) Systemic inflammation and remote organ damage following bilateral femur fracture requires Toll-like receptor 4. *Am. J. Physiol.* In press.

50. Wright SD, Levin SM, Jong MT, Chad Z, Kabbash LG. (1989) CR3 (CD11b/CD18) expresses one binding site for Arg-Gly-Asp-containing peptides and a second site for bacterial lipopolysaccharide. *J. Exp. Med.* 169:175-83.

51. Hampton RY, Golenbock DT, Penman M, Krieger M, Raetz CR. (1991) Recognition and plasma clearance of endotoxin by scavenger receptors. *Nature.* 352:342-4.

52. van Oosten M, van Amersfoort ES, van Berkel TJ, Kuiper J. (2001) Scavenger receptor-like receptors for the binding of lipopolysaccharide and lipoteichoic acid to liver endothelial and Kupffer cells. *J. Endotoxin. Res.* 7:381-4.

53. Muro M et al. (1997) Role of CD14 molecules in internalization of *Actinobacillus actinomycetemcomitans* by macrophages and subsequent induction of apoptosis. *Infect. Immun.* 65:1147-51.

54. Devitt A et al. (2004) Persistence of apoptotic cells without autoimmune disease or inflammation in CD14$^{-/-}$ mice. *J. Cell Biol.* 167:1161-70.

55. Vodovotz Y et al. (2005) Mathematical simulations of sepsis and trauma. *Proceedings of the 11th Congress of the European Shock Society.* In press.

56. Vodovotz Y et al. (2005) *In silico* models of acute inflammation in animals. *Shock.* In press.

57. Molina PE. (2005) Neurobiology of the stress response: contribution of the sympathetic nervous system to the neuroimmune axis in traumatic injury. *Shock* 24:3-10.